

A Novel approach to Robotic Cardiac Surgery using Haptics and Vision

Christopher W. Kennedy, Tie Hu, Jaydev P. Desai

Program for Robotics, Intelligent Sensing, and Mechatronics (PRISM) Laboratory

3141 Chestnut Street, MEM Department, Room 2-115

Drexel University, Philadelphia, PA 19104, USA

Email: {cwk, tie, desai}@coe.drexel.edu

Andrew S. Wechsler and J. Yasha Kresh

Department of Cardiothoracic Surgery

Medical College of Pennsylvania, Hahneman University School of Medicine

245 North 15th Street, MS-111

Philadelphia, PA 19102-1992

Email: {Andrew.Wechsler, j.yasha.kresh}@drexel.edu

Abstract

Cardiovascular disease is one of the leading causes of death in the United States and also a major disease worldwide. Over 700,000 coronary artery bypass graft (CABG) procedures are performed annually all around the world, of which 350,000 are performed in the United States. The use of mechanical stabilizers in the CABG procedures can cause irreversible local damage by traumatizing the underlying microcirculation. The primary goal of this research is to develop effective haptic and visual servoing methods for interacting with moving deformable structures. The potential application of this research is in the area of cardiac surgery. One of the primary applications will involve the elimination of mechanical stabilizers by servoing on the moving target. We present in this paper the results from our initial work in the area of tracking a deformable membrane using vision and providing haptic feedback to the user, based on the visual information through the vision hardware and the material properties of the membrane. In our first experiment, we track the deformation of a rubber membrane in real-time through stereo vision while providing haptic feedback to the user interacting with the reconstructed membrane through the PHANToM haptic device. In the second experiment, we verify the ability of our vision system to track a point on a surface undergoing a complex 3D motion.

Keywords: Medical Robotics, Cardiac Surgery, Haptics, Vision.

1 Introduction

Over the past thirty years of technical and surgical evolution, the approach to coronary artery bypass graft (CABG) surgery has remained principally unaltered. The advantages of performing CABG on an arrested heart provides a still and flacid field that can be manipulated easily to expose the vessels. The need for cardiopulmonary bypass (CPB) to facilitate this carries the cost and risk such as systemic inflammatory response, stroke and neurocognitive defects, and cardiac complications such as perioperative myocardial infarction [CMFL99, Ele97]. The associated concerns regarding the use of CPB in conventional CABG procedures now performed in over 750,000 procedures per year has given rise to an impetus for the development of minimally invasive beating heart surgery. These procedures necessitate that target vessels be exposed and immobilized, a maneuver that is frequently applied to the different regions of the heart for better visualization during the dissecting and anastomotic maneuvers. The real-time motion of the heart is very complex and varies with the beat frequency, rythm, contractility, and filling pressures to name a few. The use of mechanical stabilizers to isolate and immobilize the surface region of the heart is not without its limitations such as hemodynamic deterioration, arrythmia induction requiring inotropic support. Consequently, the use of mechanical stabilizers leads to a poor immobilization of the surgical field inspite of significant forces of traction and retraction used with these devices.

The primary goal of these studies is to develop an effective haptic (sense of touch) and visual servoing methods with the long term goal of eliminating the need for mechanical stabilizers and extracorporeal support for CABG procedures. This will effectively create a stationary operative site for the surgeon performing the procedure using haptic and visual feedback. Towards achieving the goal of relative immobilization, a set of experiments were designed for tracking a deformable membrane and providing haptic feedback to the user based on the vision information and the material properties of the membrane.

The use of vision feedback to represent the overall model of the local area of interest in a beating heart while interacting with the membrane using a finite element model creates a realistic haptic interaction with the deformable surface. An important challenge facing the development of such a system is the realistic modeling of the myocardial surface motion. Several deformable models of soft-tissue have been explored, including mass-spring models [NT98], and the more realistic, yet more computationally expensive finite element models [ZC00, FTBS01, KGPG96, Del98, SCA99].

A major constraint for any virtual surgical system is the real-time calculation of the various parameters necessary for a visually and haptically realistic experience. For a more realistic visual experience, images must be updated at a rate greater than 20 frames per second, and preferably around 200 frames per second [AH00]. Haptic systems require a much higher update rate of the sensing area, at least 500 Hz but preferable around 1000 Hz [AH00]. The disparity in the update rates for visual and haptic data suggest that the ideal robotic surgical system should be a multi-frequency system to efficiently use the computational resources [AH00, Bur00]. Numerous methods have been considered for performing the necessary calculations for virtual surgery in real-time [PLLW99, ZC00, Del98, SCA99, BG00, AH98, CT00, ML01, JP99]. A plausible approach that requires local deformation information would be appropriate in order to calculate the contact forces felt by the surgeon during the procedure [ML01]. The use of visual information for tracking the deformation of surfaces has also been studied extensively [VBR⁺99, ZK00].

2 System Description

The testbed for carrying out these experiments consists of a PHANToM haptic interface device (Sensable Technologies, Inc.), seven degree of freedom PA-10 robot arm system (Mitsubishi Heavy Industries, Ltd.), 6-axis force/torque sensor model Gamma F/T, (ATI Industrial Automation), and a pair of micro-cameras (Elmo, Canada). The experimental testbed enables the acquisition of image data from a deformable object and transmission of data to and from the PHANToM haptic device. The first generation prototype is designed such that it allows a pair of micro-cameras to observe the deformation of a rubber membrane. The deformation is controlled and measured precisely by the robotic arm, while the force data is acquired from the force/torque sensor attached to the robot manipulator end-effector. The force sensor is used as an external verification tool to compare with the force data computed from our vision setup. The results from the computed force values is displayed on the haptic device and updated in real-time at 30Hz. Figure 1 depicts the experimental system consisting of a robotic arm, deformable membrane, two micro-cameras, and a force sensor device.

Vision: The vision system comprises of two micro-cameras in a fixed configuration, with image data being acquired from each camera simultaneously. The apparatus allows a fixed stereo rig consisting of the two micro-cameras to view a circular deformable surface (see Figure 1). The surface has an inscribed array of dots (details in Section 3) that are used to calculate the contact

forces.

Robot Arm and Controller: The robot arm (see Figure 1) is used to control the deformation of the membrane and simulates the pseudo-random movement of the mock heart model attached to its end-effector. The robot arm has 7-degrees of freedom and an open controller architecture. The four layer control architecture is made up of the robot arm, servo controller, the motion control card, and the upper control computer. The control software is developed using Visual C++.

Haptic Device: The haptic device consists of a PHANToM Model 1.5A. This model has six degrees of position feedback and 3 degrees of force feedback. Haptic rendering is performed using Visual C++ and the Ghost SDK (developed by Sensable). Force calculations are performed at 1000 Hz based on the surface deformation measured by the vision system. The membrane is represented visually in the virtual environment using OpenGL, which is updated at a rate of approximately 30 Hz. The user is able to interact with the virtual deformable surface through the PHANToM device and experiences the same forces as those applied by the robot arm on the membrane.

3 Vision System

The stereo-vision system was designed to provide real-time tracking of points on the surface of any deformable object. The location of these points is used for calculation of contact forces on the surface. This requires: 1) accurate calibration of each camera's internal and external parameters, as well as the baseline of the stereo-rig, 2) a method of performing the correspondence of given surface points in a sequence of images acquired by the vision system, and 3) a method of calculating the 3-dimensional location of a surface point given data acquired from a stereo image pair.

3.1 Camera Model

All measurements made by the vision system are derived using a standard pinhole camera model [TV98]. The requisite camera parameters are obtained through calibration to calculate the position of any point in space given its location in a stereo pair of images acquired by the vision system. The parameters obtained during the calibration procedure (camera focal length, aspect ratio, and projection center) enable the reconstruction of the point in three dimensional space onto the image plane of the camera (see Figure 2). Given the extrinsic parameters of the system, namely rotation matrix, R , and translational vector, T , the location of a given point(s) in space is calculated by triangulation.

These calculations give the location of a point relative to the left camera reference frame, with its origin at the camera's focal point, and locating the positive z -axis normal to the image plane. Since the orientation of the camera reference frame is unknown, an additional calibration step is required to find the extrinsic parameters of the left camera, *i.e.*, R and T between the left camera reference frame and a known world reference frame. The location of the calculated point relative to the new reference frame can then be derived by extrinsic camera parameters (using R and T). Since the relative position measurement is of interest, it is not necessary to estimate the translational vector between the left camera reference frame and the world frame.

3.2 Image Rectification

Using the geometric constraints of the stereo rig and the calibration parameters, the search for corresponding points in a stereo image pair is reduced to a one dimensional search. This is accomplished by projecting both image planes onto a common plane that is parallel to the baseline of the stereo rig. The search for point correspondences is then performed along a single scan line [TV98, PD96, AH88].

3.3 Object Tracking

In one set of experiments, an array of circular dots attached to the surface were tracked by the stereo vision system. The array of dots were made to simulate the location of nodes in a finite element mesh. The location of the dots in the image is computed using standard blob analysis techniques [TV98], and the centroid of each dot is used to track the 3-D position of the corresponding node point on the display. In another set of experiments, a correlation tracking algorithm is implemented to track specific points on a textured surface.

3.4 Stereo Vision Algorithm

The starting point in the stereo vision algorithm is to generate the necessary lookup tables for mapping from the original image plane to the rectified plane. This allows intensity values in the rectified image plane to be computed through bilinear interpolation of the closest points in the original image. An arbitrary point on the image is selected for tracking and a 20×20 pixel window of surrounding intensity values is found for this point. Once this window is found, the tracking loop is initiated. The point is located in the original left image through SSD correlation. The image coordinates of this point is then transformed to the rectified image coordinates via an assigned lookup table. An SSD correlation is performed for the point in the rectified right image.

The rectification process narrows this search to a single scanline, which is the vertical component of the points location in the left image. The 3D location of the point is then found by triangulation. Finally, the correlation window is updated to the current surrounding intensity values of the point in the left image.

4 Haptic Interaction

Haptic feedback allows a user to experience the sense of touch of remote objects not in direct contact with the human hand. For a realistic haptic experience, contact forces must be communicated to the haptic device at a rate of at least 500 Hz. Accordingly, the PHANToM provides the haptic feedback and the vision system provides the force sensation of a deforming object. Force estimation through vision is computed based on the modulus of elasticity of the membrane and the deformation recorded by a pair of micro-cameras. The goal being to model a deformable surface using vision information and allowing the user to interact in a realistic way with the surface.

Ultimately the goal is to use these haptic interactions in minimally invasive procedures. In particular, the haptic feedback device can guide the arm of a robot to the desired location and relay the interaction of the tactile sensors at its tip to the operator. The algorithms developed in this work address a number of critical issues, such as: 1) a physical model for the surface that accurately simulates the actual forces experienced by the operator, 2) a means of haptically and visually rendering the deformable membrane intended to create a realistic interaction experience, and 3) a collision detection scheme that warns the operator when contact is made with the surface.

4.1 Surface Model - Force Calculation

In the experiments, the surface deformation is computed by a closed-form force-displacement relationship for a circular membrane with fiducials at known locations. This relationship is based on a concentrated load, W , applied over a small area [YB01]. The notation for this expression is shown in Figure 4 and the relationship is given by:

$$y = \frac{-3W(a^2 - p^2)^2(1 - \nu^2)}{4E\pi a^2 t^3} \quad (4.1)$$

where y is the displacement of the membrane at the load point, E is the modulus of elasticity, t is the thickness of the membrane, ν is the poisson's ration, a is the radius of the membrane, and p is the radial distance of eccentric loading. The general expression for the deflection due to the

applied load W at an arbitrary point, s , on the membrane is given by:

$$y = \frac{-3W(1 - \nu^2)}{4E\pi t^3} \left[\frac{p^2 r_2^2}{a^2} - r_1^2 \left(1 + 2 \ln \frac{pr_2}{ar_1} \right) \right] \quad (4.2)$$

Using this approach, force calculations at each node in response to the applied deformation on the membrane is obtained by the stereo vision system using Equation (4.1) and the material properties of the membrane. In the experimental setup, the computed forces by the vision system is compared to the force measurements by an actual force sensor attached to the tip of the robot arm (see Figure 1).

4.2 Collision Detection

For a realistic haptic experience, it is necessary to detect the collisions between the haptic interface device and the rendered deformable surface. The stylus of the PHANToM is represented as a single point in the graphic display. The task of the collision detection algorithm is to determine when the stylus (point) is in contact with any of the segments of the surface defined by the node locations. The steps in the collision detection algorithm are enumerated below.

1. During each iteration of the servo loop, the distance between the current PHANToM position and each node is calculated (for these experiments, the surface is represented by 47 nodes, 31 of which by the dots on the membrane and 16 on the boundary, which are assumed to remain stationary).
2. The distances between the nodes and the PHANToM are arranged in ascending order, the first three elements of this list are the three closest nodes to the PHANToM.
3. The collision of the PHANToM with the area enclosed by these nodes is found by calculating the angles between the lines between each node and the PHANToM; if the sum of these angles is equal to $2\pi \pm \epsilon$, a collision is identified.
4. The force sent to the PHANToM is found through an interpolation function based on the calculated force value at each node.

5 Experiments

5.1 Real-Time Force Estimation for a Deformable Membrane

The goal of the first set of experiments was to verify that the vision system can correctly measure both the deformation and the forces applied to a deformable membrane. The deformation

of the deformable membrane is measured by tracking an array of dots attached to its surface. The centroid of each dot represents a node on the surface that can then be used to reconstruct the surface both visually and haptically in a virtual environment. A sample of a stereo pair of images from this experiment is shown in Figure 5.

The robot is positioned in such a way that it deforms the membrane in a direction normal to the contact surface. The deformation of the membrane is then progressively increased in 0.5 mm increments (from 0 - 5 mm). Concurrently, a 6 degree of freedom force sensor attached to the robot end-effector measures the forces experienced by the robot while deforming the membrane. The stereovision apparatus is positioned approximately 250mm from the membrane to enable real-time acquisition of the dots fixed to the membrane.

In order to calculate the surface force, apriori knowledge of the material properties is needed. In these sets of experiments, an idealized deformable membrane (epicholohydrin rubber with poisson's ratio, 0.45 and the modulus elasticity, 27.2 MPa is used). The radius of the membrane is 39mm, with a total of 31 dots positioned at 15mm interval horizontally and 10mm interval vertically.

The representative results from tracking the displacement of the center node of the mesh are shown in Figure 6. There is a good match between the displacement of the node as measured by the vision system and that computed from the forward kinematics of the robot arm. The results for the force measurements made by the vision system and the force sensor mounted on the robot arm are shown in Figure 7. As seen, the force computed by the vision system (based on the observed displacement of the membrane at a node) and those obtained from the force sensor attached to the robot tool tip is remarkable in its similarity, considering the disparate methods for estimating interaction force.

5.2 Stereo Tracking of a Point on a Surface Through Correlation

In the second set of experiments, a more robust method for tracking a point on the object's surface was implemented. In these experiments, a correlation tracking method described in section 3 is used. A dense foam rubber model of the heart tissue is attached to the robot end-effector (see Figure 9) and the x , y , and z motion of the robot tip is commanded to move in a prescribed manner ($x(t) = 10 \cos t$, $y(t) = 10 \sin t$, and $z(t) = 10(\cos t + \sin t)$). The vision system is used to track a point on the model surface while the robot end-effector is made to move at a rate of approximately 50mm/s.

A sample of the stereo image pair acquired by the vision system is shown in Figure 8. The black

cross-hair locates a point (phantom of a coronary epicardial vessel) tracked by the vision system in each image. The results of this experiment are shown in Figure 9. The figure clearly depicts an excellent matching of the tracking algorithm with the robot motion.

Using a pulsatile beating heart model, a correlation based tracking algorithm is implemented and the recorded motion of the representative point is expectedly a more complex (see Figure 10 for a pair of stereo images and Figure 11 for the complex motion).

6 Conclusions

A vision assisted haptic interaction system capable of reconstructing a deformable surface in a virtual environment is implemented. This system has many potential applications in virtual training and endoscopic/laparoscopic surgery, where depth and haptic information are generally lacking. The experiments described are very encouraging and verify the ability to: 1) track the deformation of a surface in real-time based on the 3D movement of fixed points on the surface and render the membrane in real-time and provide haptic feedback to the user and 2) implement a robust tracking algorithm that is capable of accurately tracking the location of such points on a textured surface such as a human organ.

A natural progression of these experiments is to implement a more realistic physical modeling of the deformable surface of the beating heart. This work has several applications in robot-assisted surgery in the areas of cardiothoracic procedures, gastrointestinal surgery, and neurosurgery. In order to achieve a virtually arrested image-driven cardiac surface immobilization, a high computing capacity will be required to compensate for the highly variable cardiac motion patterns. As the surgeon works on a motion-free image, the target surface remains mobile, requiring that the robot correct automatically for the spatial deviation. Clearly, computer enhanced surgery and in particular endoscopic beating heart coronary artery bypass grafting is in its infancy. Image guided techniques for multivessel grafting remain a challenge worthy of pursuit. It is conceivable that access through the right chest or transabdominal approach will allow greater range of robotic telemanipulation and control.

Acknowledgement

We gratefully acknowledge the support of American Heart Association grant: 0160368U and National Science Foundation grant: EIA-0079830 for this work.

References

- [AH88] N. Ayache and C. Hansen. Rectification of images for binocular and trinocular stereo vision. In *9th International Conference on Pattern Recognition*, volume 1, pages 11–16, 1988.
- [AH98] Oliver R. Astley and Vincent Hayward. Multirate haptic simulation achieved by coupling finite element meshes through norton equivalents. In *Proceedings of 1998 IEEE International Conference on Robotics and Automation*, pages 989–994, 1998.
- [AH00] O. R. Astley and V. Hayward. Design constraints for haptic surgery simulation. In *Proceedings of 2000 IEEE International Conference on Robotics and Automation*, pages 2446–2451, 2000.
- [BG00] Daniel Bielser and Markus H. Gross. Interactive simulation of surgical cuts. In *Proceedings of The Eighth Pacific Conference on Computer Graphics and Applications, 2000*, pages 116–125, 2000.
- [Bur00] Grigore C. Burdea. Haptics issues in virtual environments. In *Computer Graphics International Proceedings, 2000*.
- [CMFL99] R. G. Cohen, M. J. Mack, J. D. Fonger, and R. J. Landreneau. *Minimally invasive cardiac surgery*. Quality Medical Publishing Inc., 1999.
- [CT00] Murat Cenk Cavusoglu and Frank Tendick. Multirate simulation for high fidelity haptic interaction with deformable objects in virtual environments. In *Proceedings of 2000 IEEE International Conference on Robotics and Automation*, pages 2458 – 2465, 2000.
- [Del98] H. Delingette. Toward realistic soft-tissue modeling in medical simulation. *Proceedings of the IEEE*, 86(3):512–523, March 1998.
- [Ele97] J. A. Elefteriades. Mini-CABG: A step forward or backward? The “pro” point of view. *J Cardiothorac Vasc Anesth*, 11(5):661–668, 1997.
- [FTBS01] Anrea O. Frank, Alexander Twombly, Timothy J. Barth, and Jeffrey D. Smith. Finite element methods for real-time haptic feedback of soft-tissue models in virtual reality simulators. In *Proceedings of 2001 IEEE Conference on Virtual Reality*, pages 257–263, 2001.

- [JP99] D. James and D.K. Pai. Artdefo, accurate real time deformable objects. In *Computer Graphics (ACM SIGGRAPH 1999 Conference Proceedings)*, pages 65–72, 1999.
- [KGPG96] Erwin Keeve, Sabine Girod, Paula Pfeifle, and Bernd Girod. Anatomy-based facial tissue modeling using the finite element method. In *Proceedings of the 1996 IEEE Conference on Visualization*, pages 21–28, 1996.
- [ML01] C.A. Mendoza and C. Laugier. Realistic haptic rendering for highly deformable virtual objects. In *Proceedings of 2001 IEEE Conference on Virtual Reality*, pages 264 – 269, 2001.
- [NT98] L.P. Nedel and D. Thalmann. Real time muscle deformations using mass-spring systems. *Computer Graphics International*, pages 156–165, 1998.
- [PD96] D.V. Papadimitriou and T.J. Dennis. Epipolar line estimation and rectification for stereo image pairs. *IEEE Transactions on Image Processing*, 5(4), 1996.
- [PLLW99] D.K. Pai, J. Lang, J.E. Lloyd, and R.J. Woodham. Acme, a telerobotic active measurement facility. In *Proceedings of the Sixth Intl. Symp. on Experimental Robotics*, 1999.
- [SCA99] Herve Delingette Stephane Cotin and Nicholas Ayache. Real-time elastic deformations of soft tissues for surgery simulation. *IEEE Transactions on Visualization and Computer Graphics*, 5(1):62–73, 1999.
- [TV98] E. Trucco and A. Verri. *Introductory Techniques for 3-D Computer Vision*. Prentice Hall, 1998.
- [VBR⁺99] S. Vedula, S. Baker, P. Rander, R. Collins, and T. Kanade. Three-dimensional scene flow. In *International Conference on Computer Vision*, pages 722–729, 1999.
- [YB01] W. C. Young and R. G. Budynas. *Roark’s formulas for stress and strain*. McGraw Hill, 2001.
- [ZC00] Yan Zhuang and John Canny. Haptic interaction with global deformations. In *Proceedings of 2000 IEEE International Conference on Robotics and Automation*, pages 2428–2433, 2000.

- [ZK00] Y. Zhang and C. Kambhamettu. Integrated 3d scene flow and structure recovery from multiview image sequences. *Computer Vision and Pattern Recognition*, pages 674–681, 2000.

List of Figures

- Figure 1: The experimental system for visual and haptic servoing of the deformable membrane.
- Figure 2: Camera model for stereo vision system. The intersection of rays drawn through each camera's focal point and a scene point P gives the point's location in 3D space.
- Figure 3: Flowchart for stereo correlation tracking algorithm.
- Figure 4: A theoretical model for membrane deformation for a load, W , concentrated on an area of radius, r_o .
- Figure 5: Stereo pair of images (left and right camera) acquired by vision system for tracking the deformation of a rubber membrane.
- Figure 6: Results of the measured displacement of the center node of the mesh by the vision system along with the displacement of the same node by the Mitsubishi robot.
- Figure 7: Results of the force measurements from the vision system and the force sensor due to membrane deformation.
- Figure 8: Stereo pair of images acquired by vision system for tracking a point on the surface of a heart model using correlation.
- Figure 9: Results of the correlation tracking experiment.
- Figure 10: Stereo pair of images acquired by vision system for tracking a point on the surface of a realistic heart model.
- Figure 11: Results of the tracking of a point on a realistic heart model.



Figure 1:

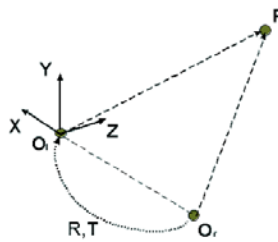


Figure 2:

Stereo Correlation Tracking Algorithm

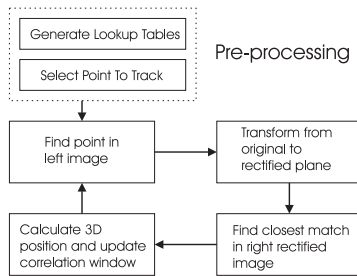


Figure 3:

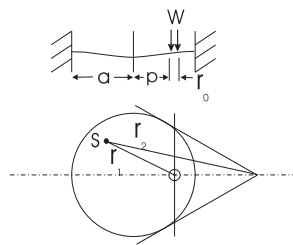


Figure 4:

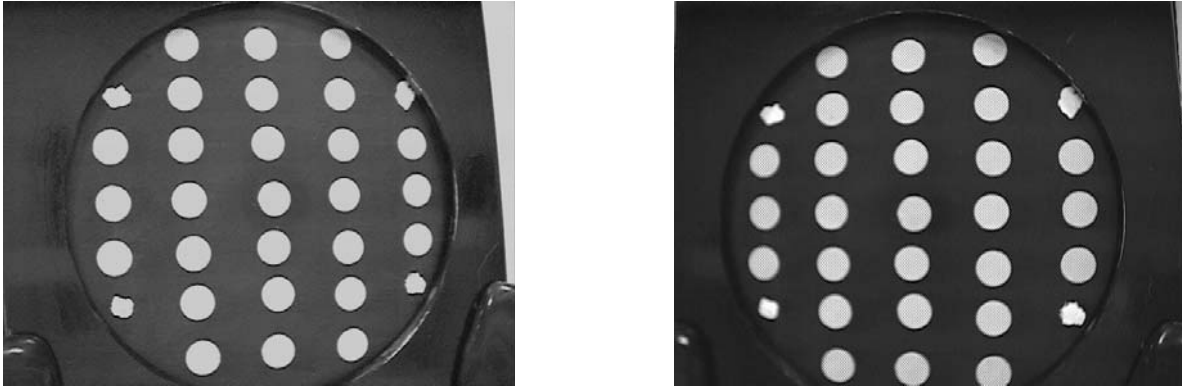


Figure 5:

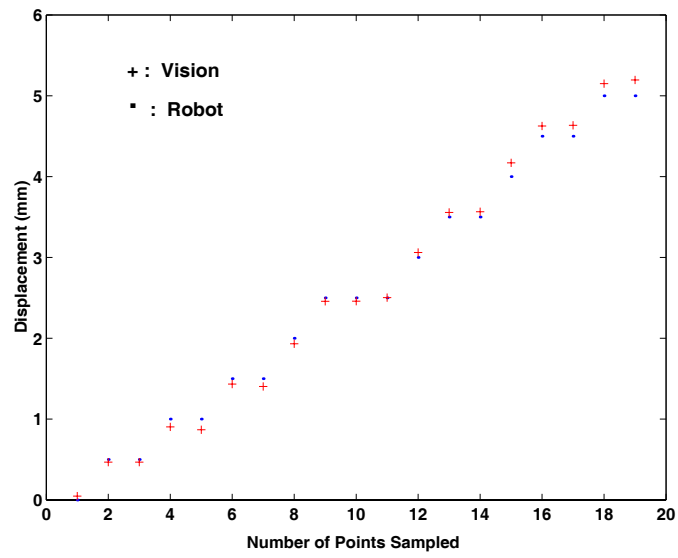


Figure 6:

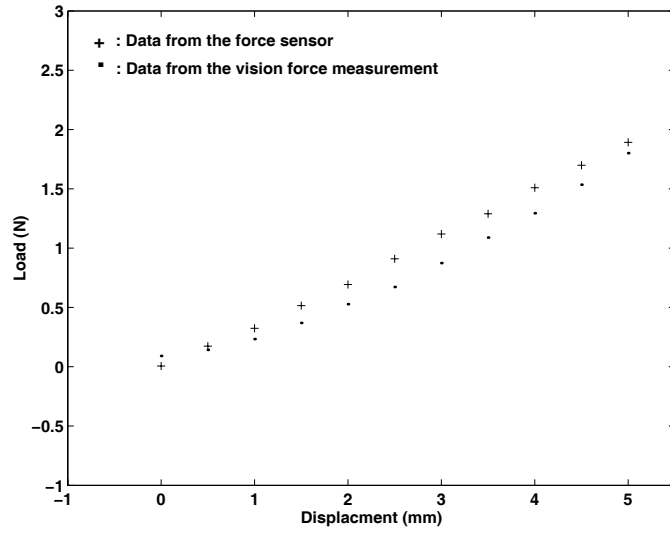


Figure 7:



Figure 8:

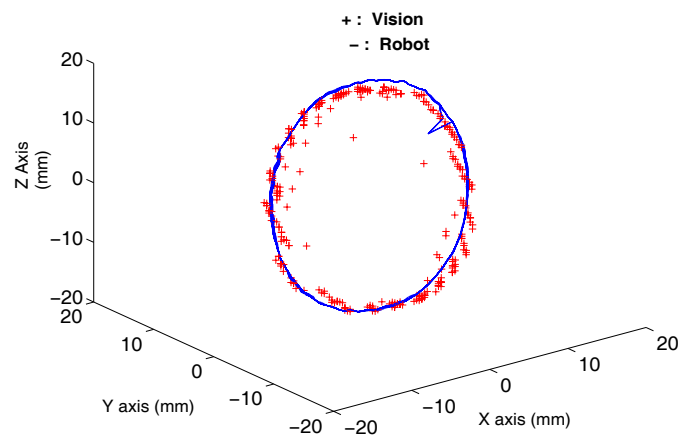


Figure 9:

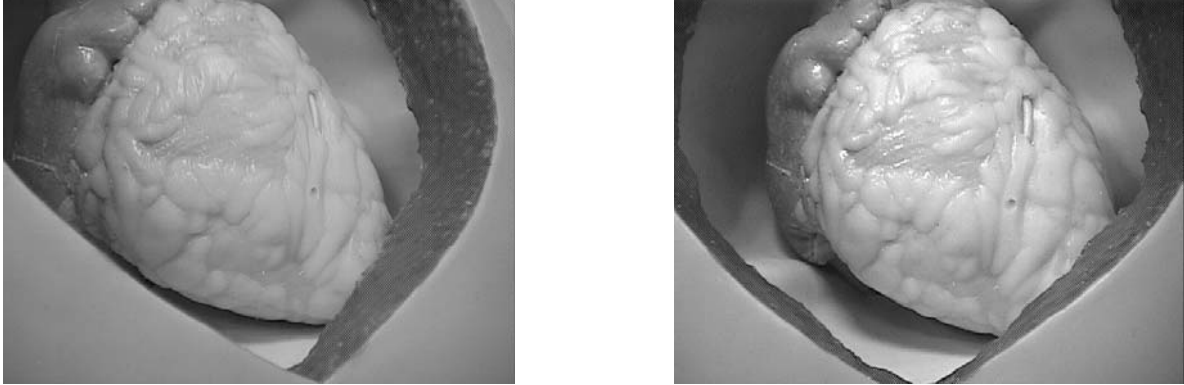


Figure 10:

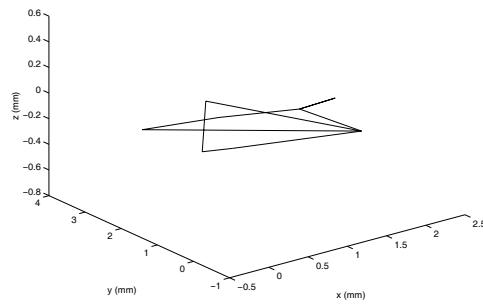


Figure 11: